J. Dairy Sci. 108:257–271
https://doi.org/10.3168/jds.2024-25493

Effects of high-temperature, short-time pasteurization on milk and whey during commercial whey protein concentrate production

Joanna Haas,[1] Bum Jin Kim,[2] Zeynep Atamer,[1] Chao Wu,[3] and David C. Dallas[1,2]*
[1]Department of Food Science and Technology, College of Agricultural Sciences, Oregon State University, Corvallis, OR 97331
[2]Nutrition Program, School of Nutrition and Public Health, College of Health, Oregon State University, Corvallis, OR 97331
[3]Hilmar Cheese Company, Hilmar, CA 95324

ABSTRACT

Two pasteurization steps are often used in the preparation of whey protein concentrate (WPC) before evaporation into a dry product. The Pasteurized Milk Ordinance in the United States requires that raw bovine milk be pasteurized using a process that meets minimum heat treatment requirements to achieve reductions in pertinent microorganisms. In addition, WPC produced from USDA-approved plants must comply with CFR subpart B §58.809, which dictates that all fluid whey used in the manufacture of dry whey products shall be pasteurized before being condensed. These heat treatments are effective at inactivating the most thermally resistant bacterium, such as *Coxiella burnetii*; however, they can also alter milk proteins, inducing denaturation, aggregation, and reduced bioactivity. Though the impact of thermal treatments on whey proteins has been examined, the specific influence of 2 HTST pasteurization steps on the retention of proteins in WPC remains unknown. This study aimed to investigate the effect of commercial-scale HTST pasteurization of both raw milk and the resulting sweet whey on the products' overall protein profile. We analyzed 3 distinct batches of raw milk (RM) and the corresponding pasteurized milk (PM), resulting whey (RW), and pasteurized whey (PW) produced at commercial scale. Assessments of denaturation were conducted through solubility testing at pH 4.6 and hydrophobicity evaluation via anilinonaphthalene-1-sulfonic acid assay. Additionally, ELISA, PAGE, and liquid chromatography tandem MS (LC-MS/MS) were employed to compare the retention of key bioactive proteins before and after each HTST pasteurization step. The percentage of soluble whey protein decreased from RM to PM and from RW to PW, but no significant differences were observed via hydrophobicity assay. The ELISA revealed a significant reduction in key bioactive proteins, such as lactoferrin, IgA, and IgM, but not IgG, after HTST pasteurization of RM and RW. The PAGE and LC-MS/MS results revealed a significant decrease in the retention of lactoferrin and key milk fat globular membrane proteins, such as xanthine dehydrogenase oxidase/xanthine oxidase, lactadherin, and fatty acid binding protein. Additionally, xanthine oxidase activity was significantly reduced after HTST pasteurization of milk and whey. This research helps to identify the limitations of the current processing techniques used in the dairy industry and could lead to innovation in improving the retention of bioactive proteins.

Key words: thermal processing, cow milk, dairy, proteomics, pasteurized milk ordinance

INTRODUCTION

Whey protein concentrate (**WPC**) is a dry powder sold as-is or added to other food items to enhance nutritional value and provide functionality (e.g., foaming, gelation; Kilara, 2015; Pires et al., 2021). Whey protein concentrate is primarily derived from the whey byproduct of cheesemaking (a.k.a., sweet whey) but may also be produced via microfiltration of milk or from acid-coagulated dairy products (O'Regan et al., 2009; Early, 2012). Typically, whey undergoes a series of processing steps to achieve a final protein concentration of 35% to 80% before being evaporated into a powder product (O'Regan et al., 2009; Early, 2012; FDA, 2024). These steps include centrifugation to remove residual fat, ultrafiltration (10–20 kDa), and diafiltration (O'Regan et al., 2009; Early, 2012; Schuck et al., 2016; Pires et al., 2021; Patel et al., 2022).

The production of WPC for human consumption in the United States must adhere to federal regulations if its product is intended for commercial sales. The Pasteurized Milk Ordinance (**PMO**) was created in 1924 by the United States Public Health Services (now the Food and Drug Administration) to ensure the safety and quality of milk and milk-derived products (FDA, 2019). The PMO section 16p, as well as 21 CFR184.1979 c(b)(3), declare that whey must be derived from milk that

Received July 24, 2024.
Accepted August 28, 2024.
*Corresponding author: dave.dallas@oregonstate.edu

The list of standard abbreviations for JDS is available at adsa.org/jds-abbreviations-24. Nonstandard abbreviations are available in the Notes.

has been pasteurized (IMNRC, 2003; FDA, 2019, 2024). Additionally, USDA-approved facilities must follow 7 CFR subpart B §58.809, which states that liquid whey must also be pasteurized in the facility in which it is dried (USDA, 2012). However, acid whey with a pH of <4.6 or titratable acidity of >0.40% is exempt from these rules (USDA, 2012; FDA, 2019). High-temperature, short-time pasteurization is the most common method of heat-treating milk and milk products due to its high throughput and efficiency in rapidly heating and cooling milk (Meunier-Goddik and Sandra, 2011). During HTST pasteurization, milk is heated to at least 72°C (161°F) for 15 s, which provides a 5-log reduction of the gram-negative bacteria *Coxiella burnetii*, the most heat-resistant pathogen in milk (Meunier-Goddik and Sandra, 2011; Mullan, 2015; Wittwer et al., 2022). The milk used to make cheese is often HTST pasteurized to meet federal safety regulations, ensure consistency, inactivate enzymes that may interfere with cheesemaking, and extend shelf life (Kelly et al., 2008; Panthi et al., 2017). Many large-volume dairy producers also pasteurize whey after cheesemaking as doing so reduces spoilage organisms, such as bacteriophages and remnants from starter cultures, as well as prevents growth of unwanted pathogens (Webb and Whittier, 1948; Pearce, 1992; Atamer et al., 2013; Briggiler Marcó and Mercanti, 2021).

Although pasteurization is essential for ensuring the safety of dairy products, it may lead to denaturation (disruption of secondary, tertiary, and quaternary structure) or degradation of key bioactive milk proteins, which can limit the product's bioactive potential for consumers. Generally, whey proteins are reversibly denatured at 55 to 65°C and irreversibly denatured at temperatures above 65 to 70°C (Qian et al., 2017; Joyce et al., 2018; Li et al., 2021). The extent of denaturation can be influenced by holding times at these temperatures, as well as ionic or pH conditions (Bernal and Jelen, 1985; Edwards and Jameson, 2014; Bogahawaththa and Vasiljevic, 2020). Individual whey protein constituents have differing thermal stabilities. For example, major whey proteins, such as β-LG, α-LA, and BSA, have higher thermal stabilities than proteins such as lactoferrin (**LF**) and Ig (Qi et al., 2015). Thermal stability is dependent on secondary, tertiary, or quaternary structure (Andoyo et al., 2018; Freire et al., 2022). In addition, mineral-binding proteins, such as LF and α-LA, can be more heat stable in their bound (holo) versus unbound (apo) forms (Burrington and Agrawal, 2012; Li et al., 2021).

The effects of pasteurization on the retention of whey proteins in milk have been previously assessed. For example, after laboratory-scale batch pasteurization (62°C, 30 min) of bovine milk, Zhang et al. (2016) observed a significant reduction (measured via liquid chromatography tandem MS [**LC-MS/MS**]) of β-LG, polymeric immunoglobulin receptor (**pIgR**), LF, fatty acid binding protein-heart (**FABP-H**), xanthine dehydrogenase oxidase and xanthine oxidase (**XDO/XO**, EC:1.17.1 .4), complement component, α-1-antiproteinase, glycosylation-dependent cell adhesion molecule 1 (**GLYCAM-1**), lactoperoxidase (**LPO**), and lactadherin (**LA**), but no reduction in heat-stable proteins, such as α-LA, α-1-acid glycoprotein, and osteopontin (**OPN**; Zhang et al., 2016). After laboratory-scale HTST pasteurization of skim bovine milk, Bogathawatha and Vasiljevic (2020) observed a 59% decrease of LF (via gel electrophoresis) but no decreased in BSA retention compared with raw milk (**RM**) controls. Similarly, after laboratory-scale HTST treatment of whole bovine milk, Liu et al. (2020b) observed a significant decrease in LF (via ELISA) and decreased abundance of proteins such as LA, LF, LPO (EC:1.11.1.7), and other minor whey proteins (via LC-MS/MS) in the serum fraction compared with untreated milk. At pilot scale, HTST treatment of skim milk decreased serum proteins, such as IgG, IgA, IgM, pIgR, and FABP-H, compared with raw skim milk controls (Zhang et al., 2021a,b). Similarly, at pilot scale, HTST treatment of whole milk decreased retention of IgG, IgA, and IgM (Liu et al., 2020a). Few studies examined the effect of HTST pasteurization at a commercial scale. Kummer et al. (1992) reported a 13% to 80% reduction of IgG (via ELISA) after (commercial-scale) HTST treatment of bovine milk from 6 commercial producers.

Only a few studies have examined the effect of pasteurizing whey on retention of specific whey proteins. In one study, HTST pasteurization (scale not specified) of whey produced by microfiltration of raw skim milk had no effect on the retention of LF, BSA, α-LA, LPO, or β-LG (measured via high performance liquid chromatography) compared with the unpasteurized control (Muuronen et al., 2021). Although not examining the effect of pasteurization on whey per se, Bogahawaththa et al. (2017) found no significant differences in the retention of BSA, α-LA, and β-LG (via gel electrophoresis and Fourier transform infrared spectroscopy) after laboratory-scale HTST treatment of whey fractions isolated by size exclusion chromatography compared with controls. No studies have examined the effect of HTST pasteurization of whey on the denaturation and retention of bioactive whey proteins.

Beyond protein concentration changes, enzyme activity can be reduced by HTST pasteurization. For example, alkaline phosphatase (EC 3.1.3.1) is deactivated by HTST pasteurization of milk (Sharma et al., 2014), and is used as an indicator of effective HTST processing (Meunier-Goddik and Sandra, 2011). LPO activity can be reduced by up to 81% after HTST treatment (USDEC, 2004; Özer, 2014; Zhang et al., 2016, 2021a,b). Studies have reported a 20% to 55% decrease in XDO/XO

activity after HTST pasteurization of milk (Sharma et al., 2014; Zhang et al., 2021a,b); however, Ozturk et al. (2019) observed no difference in the XDO/XO activity between RM and HTST-treated milk.

Other enzymes reduced by heat treatment have been reviewed previously (Deeth, 2021).

Although there is evidence that HTST pasteurization can degrade certain whey proteins in both milk and whey, no previous studies have examined the effect of the combination of HTST pasteurization applied to both milk and whey on bioactive proteins. As these combined processes are often used upstream of evaporation in the commercial production of whey protein products, there is a need to understand their impacts on the retention and degradation of bioactive proteins. This study aims to identify the effects of HTST pasteurization of milk and whey on bioactive protein retention.

MATERIALS AND METHODS

Milk Processing and Sample Acquisition

Three lots of RM, pasteurized milk (**PM**), the resulting whey (**RW**), and pasteurized whey (**PW**) were provided frozen on ice by Hilmar Cheese Company Inc. (Hilmar, CA). The RM was collected from Jersey and Holstein cows at various stages of lactation and stored at 4°C in bulk tanks. It then underwent HTST pasteurization at 72°C for 16 s, and samples were collected (PM). Following this, the PM was curdled via the addition of rennet and starter cultures (at temperatures <40°C) for commercial-scale American style cheese production, and the resulting sweet whey byproduct (RW) was collected. The sweet whey underwent a sequence of industrial purification steps, including fat separation (separator) and HTST pasteurization (72°C for 16 s), and the PW was collected (Figure 1).

Solubility Assay

The solubility method used to separate out soluble whey proteins was adapted from previous methods as outlined by Anandharamakrishnan et al. (2007), Grácia-Juliá et al. (2008), and Zhang et al. (2016), with some modifications, including solvent type, centrifuge speed, and method of protein quantification. Each solution (RM, PM, RW, and PW) was divided into two 25-g aliquots: one aliquot was adjusted to pH 4.6 via addition of 0.25 *M* HCl (0.15–1.0 mL), whereas the other was adjusted to the same final weight with ultrapure water. The pH 4.6 aliquot was centrifuged at 10,000 × *g* for 30 min at 21°C (5427 R Centrifuge, Eppendorf, Hamburg, Germany) to remove any remaining caseins or insoluble proteins and aggregates, and the supernatant was then extracted. The pH-adjusted and centrifuged sample is hereafter referred to as the soluble fraction sample (**SFS**), whereas the untreated sample is referred to as the whole sample (**WS**; Figure 1). Protein quantification of each sample was carried out via a Pierce BCA Protein Assay kit (Thermo Fisher Scientific, Waltham, MA) to determine the amount of soluble protein in the SFS relative to the amount of protein in the WS. In this assay, proteins reduce the copper ion from Cu^{2+} to Cu^{1+} via a reaction with amino acid sides chains, such as cysteine. The Cu^{1+} reacts with the bicinchoninic acid (**BCA**), resulting in a colorimetric change that can be

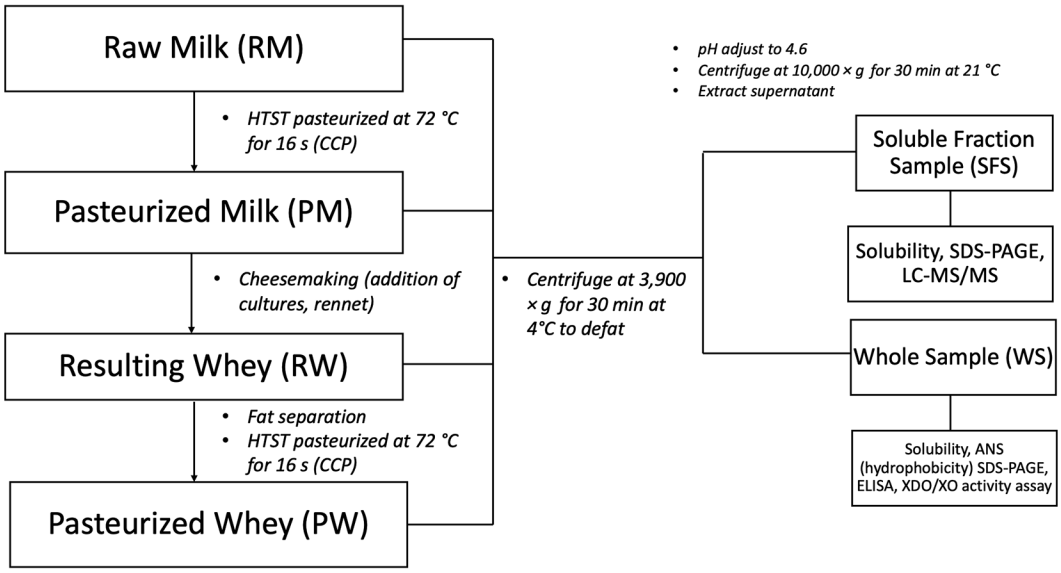

Figure 1. Flowchart of sample generation and processing. CCP = critical control point.

read via absorbance at 562 nm (Olson, 2016). Before measurement, solutions of each SFS and WS were diluted 10-fold in ultrapure water. All samples were measured in triplicate, and the entire experimental sample preparation was repeated twice to examine variation in the assay. The percentage of total protein solubility was calculated using Equation 1.

$$Total\ Protein\ Solubility\,(\%) = \frac{Conc.\ of\ pH\ 4.6\ sample\,(SFS)}{Conc.\ of\ uncentrifuged\ sample\,(WS)}, \quad [1]$$

where *SFS* is the soluble fraction sample, *WS* is the whole sample, and *Conc*. is concentration.

SDS-PAGE

Samples (both WS and SFS from RM, PM, RW, and PW) were assessed via SDS-PAGE using a Bio-Rad precast Criterion TGX 4% to 20% polyacrylamide gel. All samples were diluted to ~2 mg·mL^{-1} protein in ultrapure water. They were then prepared in reduced and nonreduced forms. Reduced samples were prepared by adding 13.2 µL of Bio-Rad Laemmli loading buffer (62.5 m*M* Tris-HCl, pH 6.8, 10% glycerol, 1% lithium dodecylsulfate, 5% bromophenol blue) and 5.5 µL of 1.0 *M* dithiothreitol (**DTT**) to 40 µL of the diluted samples before heating to 95°C for 5 min to achieve full denaturation. Nonreduced samples were prepared in the same manner, except the reducing agent (DTT) was not added. Next, ~30 µg of protein was loaded into each well. An aliquot of Precision Plus Dual Color Standard (Bio-Rad) was added to the first and last lane of the gel as a reference standard. The gel was run at 180 mV for 1 h in a Criterion cell with a running buffer of 1X Tris/Glycine/SDS (Bio-Rad). The gel was then rinsed 3 times in ultrapure water for 15 min each, stained using Bio-Rad Coomassie Brilliant Blue G-250 for 1 h and destained in ultrapure (18.2 MΩ·cm) water for 30 min. Gels were imaged using a gel imager (Odyssey 9120 Near Infrared Gel Imager, LICOR, Lincoln, NE) at 700 nm.

Anilinonaphthalene-1-Sulfonic Acid Hydrophobicity

Anilinonaphthalene-1-sulfonic acid (**ANS**) is a hydrophobic (apolar) fluorescent compound that binds to the unfolded nonpolar regions of proteins. The quantum yield of ANS increases after binding to hydrophobic portions of proteins. All of the WS samples of RM, PM, RW, and PW was diluted to create 1-mL standards ranging from 0.0625% to 1.50% protein (wt/wt) in 0.01 *M* HEPES buffer (4-(2-hydroxyethyl)-1-piperazineethanesulfonic acid, pH 7–7.5; Spectrum Chemical Mfg. Corp., New Brunswick, NJ). Protein solutions were stored at 4°C for 24 h. Each 1-mL standard was aliquoted into two 500-µL aliquots. One 500-µL aliquot served as the protein blank. The other 500-µL aliquot was spiked with 2.5 µL of 8 m*M* ANS (Spectrum Chemical Mfg. Corp., New Brunswick, NJ) in 0.01 *M* HEPES buffer. A 200-µL aliquot of each sample (sample with ANS, blank samples without ANS, and buffer blank) was aliquoted in a duplicate well of a 96-well fluorescent microplate. The plate was incubated for 15 min at 30°C with mixing at 300 rpm. Then the relative fluorescent intensity (**RFI**) was measured with a spectrofluorometer (Molecular Devices SpectraMax M2 Plus Microplate Reader, San Jose, CA) at excitation wavelength (**λ ex**) of 390 nm and emission wavelength (**λ em**) of 470 nm. The blank (including both protein and buffer) was subtracted from each measurement to obtain the final RFI value. The RFI was plotted against protein concentration, and the slope of the line (the hydrophobicity index, $\mathbf{S_0}$) was calculated by linear regression analysis.

ELISA

The presence of bovine LF, IgM, IgA, and IgG were analyzed using the ELISA method. The kits used were the Bovine Lactoferrin ELISA kit (ab274406, abcam, Waltham, MA), Bovine IgG ELISA kit (ab205078, abcam), Cow IgA kit (ab190516, abcam), and Bovine IgM kit (COV91-K01, Eagle Biosciences, Nashua, NH). The samples for the LF ELISA were diluted in assay buffer (provided in the kit) by the following amounts: RM and PM samples, 4,000-fold; RW samples, 800-fold; and PW samples, 400-fold. Samples for the IgG, IgA, and IgM ELISA were diluted in assay buffer (provided in the kit) by the following amounts: RM and PM, 40,000-fold; RW, 20,000-fold; and PW, 5,000-fold. All samples were WS and measured in duplicate.

The standard provided in each ELISA kit was spiked in each sample to determine the detection efficiency of the assay to account for any matrix effects. The concentrations provided in the LF ELISA, IgG, IgA, and IgM kits were spiked to achieve a final additional concentration in the samples of 50 ng·mL^{-1}, 20 ng·mL^{-1}, 28 ng·mL^{-1} and 28 ng·mL^{-1}, respectively. Each spike was carried out on a diluted sample of one replicate (lot) of RM, PM, RW, or PW before running the assay (Supplemental Table S1, see Notes). The calculation used to determine detection efficiency is shown in Equation 2.

$$Detection\ Efficiency\,(\%) = \frac{(Avg\ of\ Sample\ with\ Spike - Avg\ of\ Unspiked\ Sample)}{Spike\ addition\ to\ final\ concentration}. \quad [2]$$

All samples for the ELISA were measured at 540 nm on a spectrophotometer (Molecular Devices SpectraMax M2 Microplate Reader). A quadratic fit for the standard curve was constructed for each assay, and the final concentration of each unknown was determined via SoftMax software (version 7, Molecular Devices SoftMax Pro Software, San Jose, CA).

Xanthine Oxidase Activity Assay

Xanthine oxidase is an enzymatic (specifically oxidoreductase) milk fat globular membrane (**MFGM**) protein that converts xanthine into uric acid (Farkye, 2002). The presence of XDO/XO activity was measured via activity kit (Xanthine Oxidase Fluorometric Assay Kit, item no. 10010895, Cayman Chemical, Ann Arbor, MI). This assay measures XDO/XO activity via the production of the fluorescent molecule resorufin. The RM and PM samples were diluted 5,000-fold in assay buffer, and RW and PW samples were diluted 2,500-fold in assay buffer.

The standard provided in the XDO/XO activity assay kit was spiked in the samples (TS samples of RM, PM, RW, PW) to determine the detection efficiency of the assay to account for any matrix effects. We spiked 20-μU·mL^{-1} aliquots into diluted samples of 1 replicate (lot) of RM, PM, RW, and PW before running the assay (Supplemental Table S1). The calculation used to determine detection efficiency is shown in Equation 2.

The RFI of samples and standards were measured with a spectrofluorometer (SpectraMax M2 Plus Microplate Reader, Molecular Devices, San Jose, CA) at λ ex of 530 nm and λ em of 590 nm. The blank was subtracted from each measurement to get the final RFI value. A linear fit for the standard curve was constructed, and the final concentration of each unknown was determined via SoftMax software (Molecular Devices SoftMax Pro Software, San Jose, CA). Each linear regression model was constructed from the averages of each dilution across 3 lots for each sample type.

LC-MS/MS

A bottom-up proteomics approach was used to quantify the proteins in each sample via LC-MS/MS. The whey fraction of each sample was extracted as described in the previous solubility section (SFS samples only). Then samples were further prepared according to the methods of Kim et al. (2023). The approximate starting concentration of each sample was 7 μg·μL^{-1}. All samples were prepared in duplicate. A 150-μL aliquot of chilled (–20°C) ethanol (Sigma Aldrich, St. Louis, MO) was added to 30 μL of each sample at a 5:1 ratio (by volume). Samples were then vortexed, chilled at –20°C for 1 h, and centrifuged at 12,000 × *g* for 20 min at 4°C before the supernatant (containing peptides) was separated from the pellets (containing proteins). The pellets were then dried in a centrifugal evaporator for 70 min (maximum temp 37°C) at the low boiling point setting (Genevac, SP Scientific, Warminster, PA) before reconstitution in 100 μL of 50 m*M* ammonium bicarbonate (Thermo Scientific) buffer with a pH between 7 and 8 for at least 24 h at 4°C. A 2-μL aliquot of 550 m*M* DTT was added to each sample, and samples were incubated at 50°C for 50 min at 300 rpm to reduce disulfide bonds. After this, a 4-μL aliquot of 450 m*M* iodoacetamide was added to each sample, and samples were again incubated at room temperature for 60 min in the dark to alkylate thiol groups. An aliquot of 1 μg·mL^{-1} Trypsin/Lys-C (Trypsin/Lys-C Mix, Mass Spec grade, Promega, Madison, WI) was added to samples to achieve a 1:50 ratio of protease to protein. Samples were then incubated for a third time at 37°C for 16 h at 300 rpm (ThermoMixer C, Eppendorf, Hamburg, Germany) to complete digestion.

The trypsin-digested peptides were extracted from the samples via C18 solid phase extraction (5 mL tube volume, 500 mg bed weight, 45 μm particle size, Sigma Aldrich, St. Louis, MO). Cartridges were conditioned by adding 5 mL of ultrapure water, 5 mL of 80% acetonitrile (**ACN**; Merck, Darmstadt, Germany) with 0.1% trifluoroacetic acid (Merck, Darmstadt, Germany) and then another aliquot of 5 mL of ultrapure water. Samples were then loaded by adding 1 mL of ultrapure water followed by the 100-μL sample. Samples were first washed with 5 mL of ultrapure water to remove any polar constituents, such as salts, before being eluted with 5 mL 80% ACN with 0.1% trifluoracetic acid. The eluents were collected and dried in a centrifugal evaporator.

The dried samples were reconstituted in 100 μL of 3.0% ACN, 0.1% formic acid (**FA**) for 24 h at 4°C and further diluted in 3.0% ACN, 0.1% FA to ~100 ng·μL^{-1}. They were then injected into a Waters nanoACQUITY ultra-performance liquid chromatography system (Waters, Milford, MA) with a nanoEase M/Z Symmetry C18 Trap Column (100Å, 5 μm, 180 μm × 20mm; Waters) and a nanoEase M/Z Peptide BEH C18 Column (130Å, 1.7 μm, 75 μm × 100 mm; Waters). A 1-μL aliquot of each sample was loaded on the columns and separated over the course of 60 min with a flow rate of 0.3 μL × min^{-1} with the following gradient, using solvent A (99.9% ultrapure water with 0.1% FA) and solvent B (99.9% ACN with 0.1% FA): 3% to 15% B, 0 to 4.5 min; 15% to 30% B, 4.5 to 45 min; 30% to 95% B, 45 to 50 min; 95% B, 50 to 55 min; 95% to 3% B, 55 to 58 min; 3% B over 0.5 min. Then the column was re-equilibrated with 97% A for 3 min.

The sample was detected using an Orbitrap Fusion Lumos Tribrid Mass Spectrometer (Thermo Scientific, Waltham, MA) with an electrospray voltage of 2,350 V

and tube temperature of 300°C. Full scan MS spectra were acquired in positive ionization mode over an m/z range of 300 to 2,000 with a resolution of 60,000. The automatic gain control target was set to 4.0×10^5, with a maximum injection time of 50 ms, and the MS cycle time was set to 3 s. Following an MS scan, acquisition software automatically selected precursor compounds for MS/MS analysis based on the following criteria: ion-intensity threshold 5.0×10^4, charge state 2 to 8, and exclusion time 60 s. Higher energy collision dissociation-based fragmentation was performed with 30% of collision energy. All MS/MS spectra were acquired in the positive ionization and auto scan range mode by the Orbitrap at a resolution of 60,000, and the automatic gain control target was set to 5.0×10^4 for all fragmentation techniques.

Two experimental replicates of each sample were analyzed to account for variation in sample preparation. Data files were analyzed in Thermo Proteome Discoverer (v 3.1) using the Sequest HT search engine against a bovine milk protein database from UniProt containing 6,046 protein sequences (Supplemental Table S2, see Notes) and a bovine Ig database containing 79 protein sequences compiled from identified Ig peptides in previous literature (Masterson et al., 2024; Supplemental Table S3, see Notes). The library includes various peptide components of Ig, including light, heavy, and joining chains (Gorevic et al., 1985; Johansen et al., 2000; Nezlin, 2019). Cleavage sites were set to C-terminal arginine and lysine, and digestion specificity was selected as fully specific with a maximum of 2 missed cleavages. The precursor mass tolerance was set to 10 mg/kg with fragment mass tolerance of 0.1 Da. Minimum and maximum peptide length were set to 4 and 150 amino acids, respectively. Fixed modifications were set as carbamidomethylation (+57.021 Da) of cysteine. Dynamic modifications were set as methionine oxidation (+15.995 Da), serine and threonine phosphorylation (+79.966 Da) and N terminus acetylation (+42.011 Da). Only proteins identified with high confidence (q-value < 0.01) were retained for further analysis. Total protein abundances were calculated from the sum of the intensities of all peptides identified from each protein.

Statistics

Measurements for each sample type (RM, PM, RW, and PW) were compared using an ANOVA with post hoc Tukey's honestly significant difference tests (p-value <0.05). For proteomics data, volcano plots were constructed for all proteins detected in all samples of each comparison (i.e., RM vs. PM, RW vs. PW), with the 2-log fold change (from raw abundance values) plotted against −log10 P-values from Student's t-tests. All statistical analyses and visualizations were carried out in R statistical software (RStudio Version 2023.06.2+561, Posit Software PBC, Vienna, Austria).

RESULTS AND DISCUSSION

Solubility

The solubility assay used herein reliably assesses the quantity of soluble (typically non-denatured) whey proteins present in the samples. Native whey proteins remain soluble at pH 4.6, the isoelectric point of caseins; if a whey protein is insoluble at pH 4.6, it could be due to aggregation or denaturation and, therefore, loss of native structure (De Wit and Van Kessel, 1996; Ryan et al., 2013). The whey solubility for RM and PM was 22.6% and 18.9%, respectively (Table 1). The solubility values for RM and PM were reflective of the soluble whey present in the sample (as the casein content would have been precipitated out). This finding is consistent with the approximate casein/whey ratio (80:20) in bovine milk (Davoodi et al., 2016). The average whey solubility of RW and PW was 94% and 90.6%, respectively (Table 1). The increase in soluble whey protein from PM to RW is expected, as caseins were removed.

The solubility of PM was significantly lower than that of RM, and the solubility of PW was likewise significantly lower than that of RW (Table 1, $P < 0.05$). The average loss in whey protein solubility from RM to PM and RW to PW, was 16.5% and 3.62%, respectively. The solubility of whey proteins in milk and whey after thermal treatments has been previously evaluated by adjusting the pH to 4.6 and using centrifugation to remove insoluble proteins, aggregates and caseins (Morr, 1987; Pelegrine and Gasparetto, 2005; Dissanayake and Vasiljevic, 2009; Allen, 2010). However, only one of these studies has assessed solubility of whey proteins before and after HTST pasteurization of milk and sweet whey in tandem (Morr, 1987). The solubility values for our whey samples (90.6%–94%) are within the range observed by Allen (2010), who found the solubility (via BCA) of whey protein to be 93.24% to 93.93% after laboratory-scale heat treatment (76°C for 15 s) and drying. However, our values are somewhat lower than those observed by Morr (1987), who reported 95.7% to 100.6% solubility of UF sweet whey (measured via the micro-Kjeldahl and Biuret methods). Rynne et al. (2004) reported an average whey protein denaturation level of 2.8% in their PM sample (72°C for 26 s), which is lower than our observed 16.5% average loss in whey protein solubility. Their finding may differ from ours because they used a different methodology to assess native whey protein (subtracting sodium acetate-acetic acid-precipitable casein and trichloroacetic acid non-precipitable nonprotein nitrogen from the total protein; Rynne et al., 2004).

Table 1. Solubility and hydrophobicity results for raw milk (RM), pasteurized milk (PM), resulting whey (RW), and pasteurized whey (PW) samples (results expressed as mean ± SD)

	Milk samples		Whey samples	
Measured parameter	RM	PM	RW	PW
Solubility[1] (%)	22.63 ± 1.29[a]	18.89 ± 0.59[b]	93.95 ± 2.84[A]	90.55 ± 3.49[B]
Hydrophobicity[2] (S_0)	889.81 ± 87.53	991.37 ± 15.65	562.68 ± 89.58	566.77 ± 55.89

[a,b]Mean values in the same row with different superscripts differ ($P < 0.05$) significantly for RM and PM.

[A,B]Mean values in the same row with different superscripts differ ($P < 0.05$) significantly for RW and PW.

[1]Mean solubility (%) for RM, PM, RW, and PW. Values were calculated as the average of 3 separate lots (n = 3).

[2]Average hydrophobicity indices (S_0) determined via ANS hydrophobicity assay for RM, PM, RW, and PW. Values were calculated as average of the slopes of 3 separate lots (n = 3).

ANS (Hydrophobicity)

The higher the S_0, the greater the surface hydrophobicity of proteins in a sample, and a higher surface hydrophobicity can indicate increased denaturation (Latypov et al., 2008). Previously, hydrophobicity via ANS has been used to assess surface hydrophobicity of milk and whey samples (Alizadeh-Pasdar and Li-Chan, 2000; Chandrapala et al., 2015; Sharma et al., 2016). We found no significant difference in hydrophobicity index between RM and PM (Table 1). However, Sharma et al. (2016) observed a significant increase in S_0 in their milk sample treated at 73°C for 15 s (like our treatment) compared with their RM control, which they attributed to the unfolding of globular proteins. Although we did observe a numerical increase in S_0 from RM to PM, it was not significant.

Similarly, we observed no difference in S_0 between RW and PW (Table 1). Chandrapala et al. (2015) saw an increase of S_0 in raw acid whey samples (pH 7.3) when heated at 40°C for 20 min (at laboratory scale) but saw a decrease for samples heated at 90°C for the same amount of time. They proposed that the decrease was due to the dependency of the assay on the surrounding ionic conditions and destruction of potential binding sites for the fluorescent probe via thermal denaturation. Making comparisons between our study and that of Chandrapala et al. (2015) is difficult due to differing temperature treatments and material (acid whey vs. sweet whey). Alizadeh-Pasdar and Li-Chan (2000) found a significant increase of S_0 in their heat-treated (80°C for 30 min, laboratory scale) 1.5% wt/wt whey protein isolate and β-LG solutions compared with their untreated controls. The lack of increase in our study compared with that of Alizadeh-Pasdar and Li-Chan (2000) may be because we used less intense pasteurization treatments.

Gel Electrophoresis

Gel electrophoresis, specifically SDS-PAGE, was used to identify differences in the protein profile among RM, PM, RW, and PW samples. Samples were prepared in both reducing (addition of DTT) and nonreducing conditions to identify if there were any disulfide-bonded aggregates. The reduced samples had a band at 150 kDa (Figures 2 and 3), which corresponds to the reduced form of XDO/XO, as indicated previously (Beyaztaş and Arslan, 2015). The reduced form of IgG appeared as 2 separate bands at ~50 kDa and ~25 kDa, which correspond to heavy-chain and light-chain IgG, respectively (Ng et al., 2010). The IgG in the nonreduced form in all samples appeared just above 150 kDa (Figures 2 and 3). Lactoferrin appeared at ~80 kDa in the reduced form and, as a faint band, just below ~75 kDa in the nonreduced form (Figures 2 and 3). Other bands were visible at ~60 kDa (both reduced and nonreduced form), ~20 to 25 kDa (both reduced and nonreduced form), ~18 kDa (both reduced and nonreduced form) and ~14 kDa (both reduced and nonreduced form) and correspond to BSA, various caseins, β-LG and α-LA, respectively.

There were key differences between reduced and nonreduced samples. Reduced samples (across lots and sample type) did not have a band at the top of the gel, whereas nonreduced samples did (Figures 2 and 3). These bands (>250 kDa) were the most intense in RW and PW samples, specifically in the TS samples, suggesting the presence of an aggregate that is formed during cheese-make (Figure 2). The band intensity from LF in the SFS decreased across RW to PW, suggesting a loss of the native form of this protein (Figure 3). The nonreduced and reduced forms of β-LG, α-LA, BSA, and heavy-chain IgG were the same intensity from RW to PW (Figures 2 and 3). The band intensity of XDO/XO (~150 kDa) in 2 of the lots decreased in intensity from RW to PW (nonreduced sample; Figure 3b and 3c). Overall, our SDS-PAGE results align with those of Qi et al. (2015), who saw no difference in intensity between their RM whey and PM whey for β-LG, α-LA, BSA, and IgG. Furthermore, our results align with those of Bogahawaththa and Vasiljevic (2020), who observed a decrease in LF band intensity (but not BSA) in their heated skim milk compared with their raw skim milk control, as measured

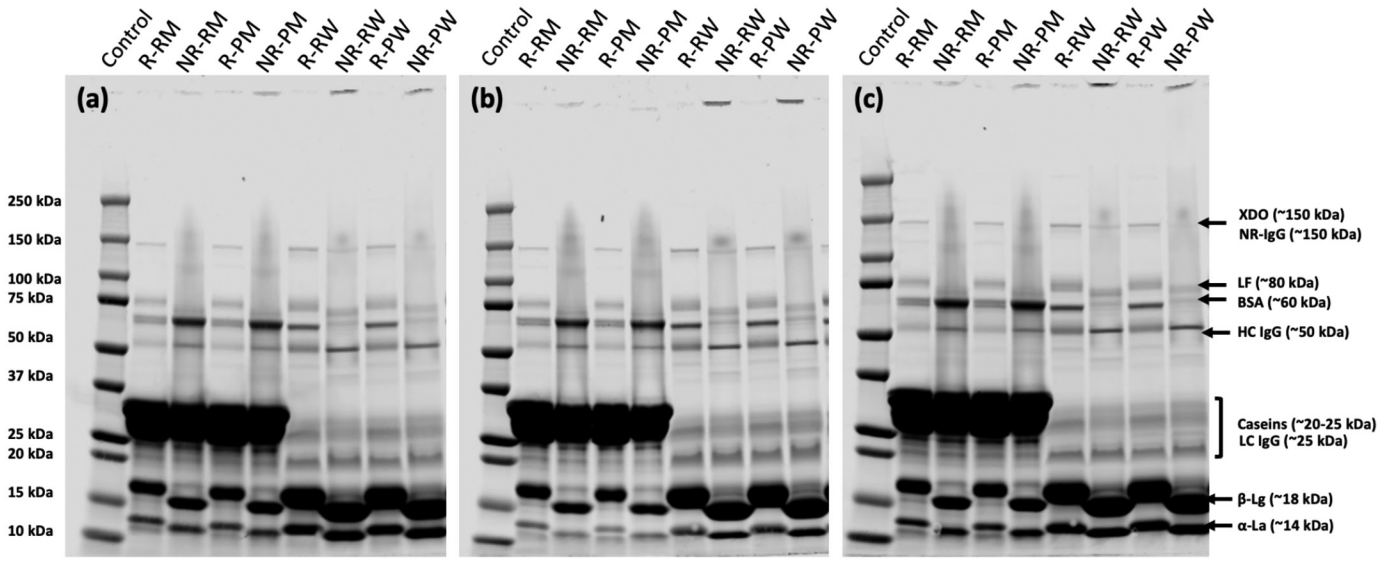

Figure 2. Results of SDS-PAGE of reducing (R) and nonreducing (NR) raw milk (RM), pasteurized milk (PM), resulting whey (RW) and pasteurized whey (PW) of whole sample (WS). (a) Lot 1, (b) Lot 2, (c) Lot 3.

by SDS-PAGE. Our results partially align with those of Zhang et al. (2021b), who observed no difference in band intensity (via SDS-PAGE) for BSA, β-LG, and α-LA, and a decrease in band intensity for LF in HTST-treated skim milk compared with their untreated control. However, unlike their study, ours not see a decrease in band intensity for heavy chain IgG.

ELISA

The percent retention of LF decreased significantly from RM to PM and from PM to RW. However, LF retention did not decrease significantly from RW to PW (Figure 4a). The percent retention of IgG did not significantly decrease across sample types (Figure 4b). The percent retention of IgA decreased from RM to PM, but was not significantly different between PM, RW, and PW (Figure 4c). The percent retention of IgM decreased significantly from RM to PM but was not significantly different between PM and RW. However, there was a significant decrease in IgM retention from RW to PW (Figure 4d). Detection efficiency for LF, IgG, IgA, and IgM ranged from 95% to 130%, 75% to 100%, 92% to 135%, and 133% to 186%, respectively (Supplemental Table S1).

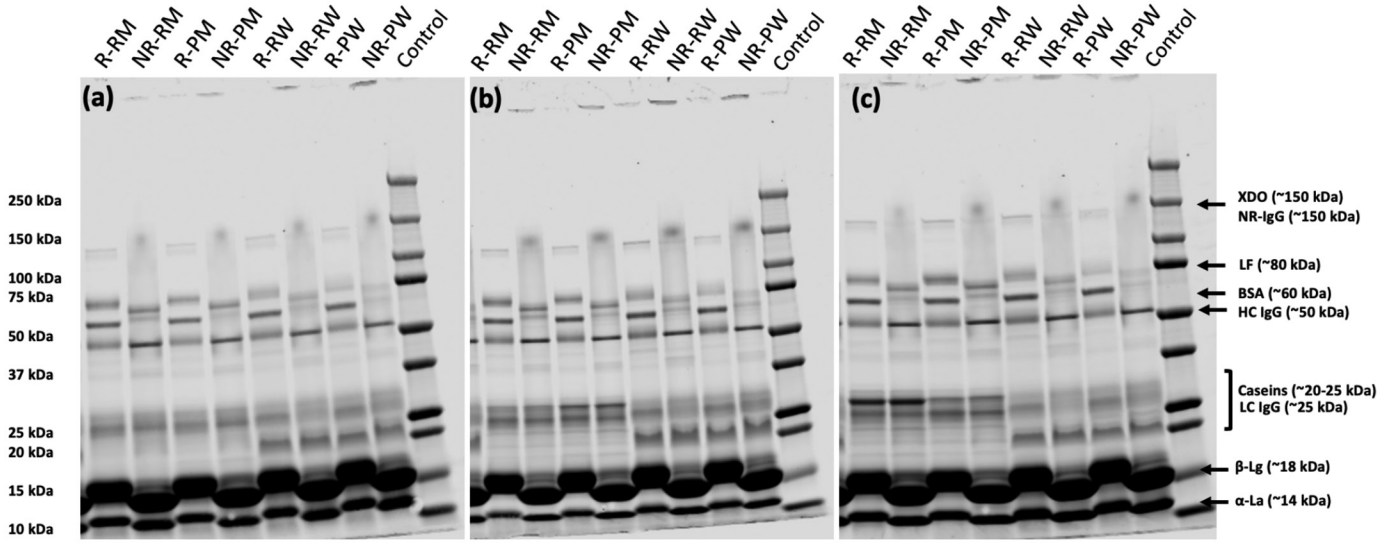

Figure 3. Results of SDS-PAGE of reducing (R) and nonreducing (NR) raw milk (RM), pasteurized milk (PM), resulting whey (RW) and pasteurized whey (PW) of soluble fraction sample (SFS). (a) Lot 1, (b) Lot 2, (c) Lot 3.

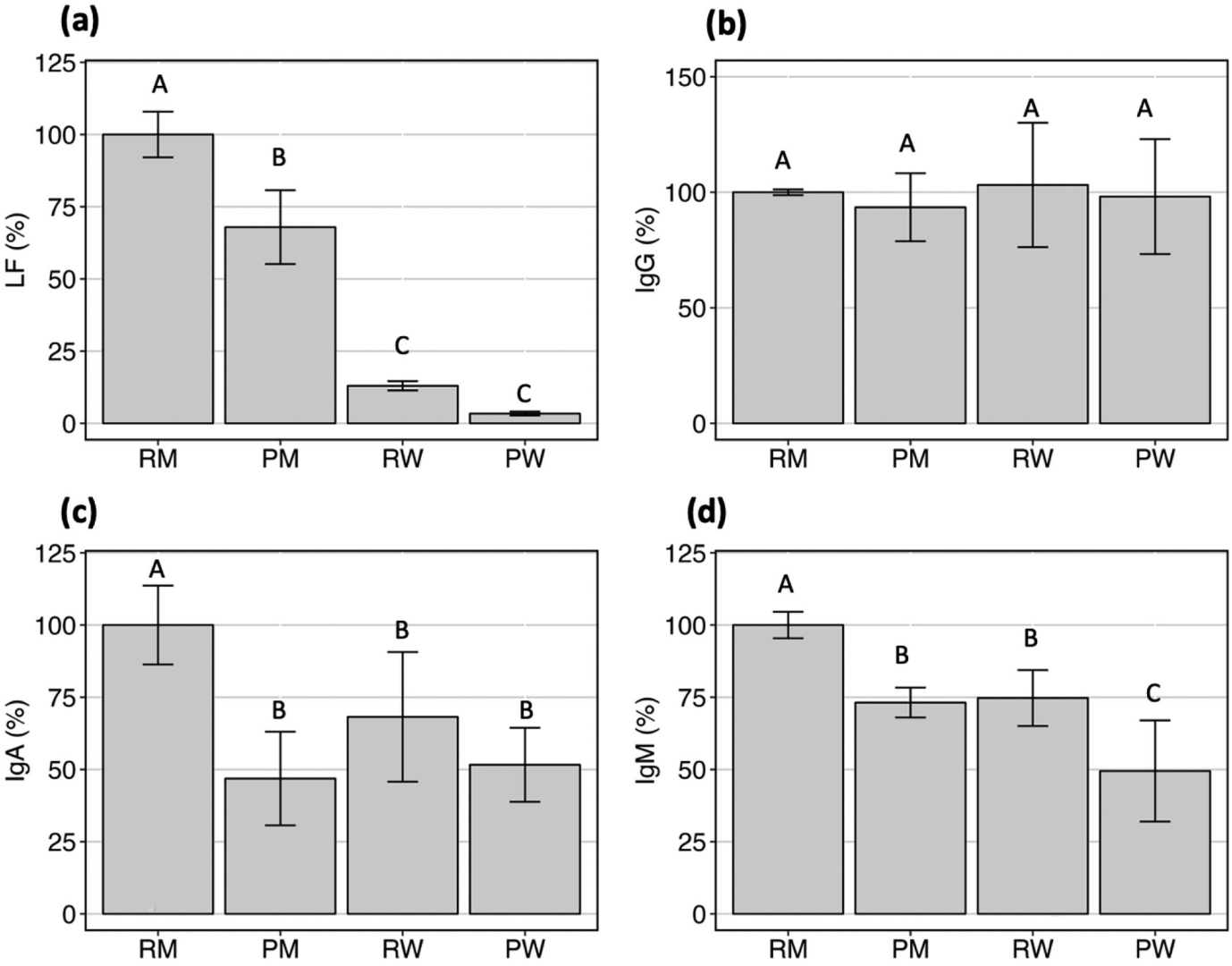

Figure 4. Percent retention (%) of select proteins for raw milk (RM), pasteurized milk (PM), resulting whey (RW), and pasteurized whey (PW) identified via ELISA. Percent retention has been calculated as the amount of protein detected divided by the amount detected in the control (RM). (a) Lactoferrin (LF), (b) IgG, (c) IgA, (d) IgM. Error bars represent SD. Significantly different samples are denoted by differing uppercase letters (A–C; Tukey's honestly significant difference test, $P < 0.05$).

Other studies have used ELISA to evaluate the retention of LF and select Ig before and after heat treatment of milk products (Kummer et al., 1992; Bogahawaththa et al., 2018; Liu et al., 2020a; Wazed et al., 2020; Zhang et al., 2021a). Our results for IgA, IgM, and LF align with those of Zhang et al. (2021a,b), who saw a decrease in retention of these proteins after HTST heat treatment of skim milk. However, unlike these researchers, we did not see a significant decrease in IgG retention (Zhang et al., 2021a). Furthermore, our IgG results do not align with those reported by Kummer et al. (1992), Liu et al. (2020a,b), and Bogahawaththa and Vasiljevic (2020), who all saw a significant decrease in IgG retention after HTST treatment of milk. However, our results do align with those of by Bogahawaththa et al. (2018), who did not see a significant decrease in native IgG retention after HTST treatment of skim milk samples. Previous research indicates that IgG is more heat stable than IgA and IgM, which could explain why we did not observe a decrease in retention for IgG (Mainer et al., 1997; Hurley and Theil, 2011).

XDO/XO Activity

We found that XDO/XO activity decreased ~15% from RM to PM, but not significantly (Figure 5). However, we observed a significant decrease in XDO/XO activity retention from PM to RW samples (25%–45% retention

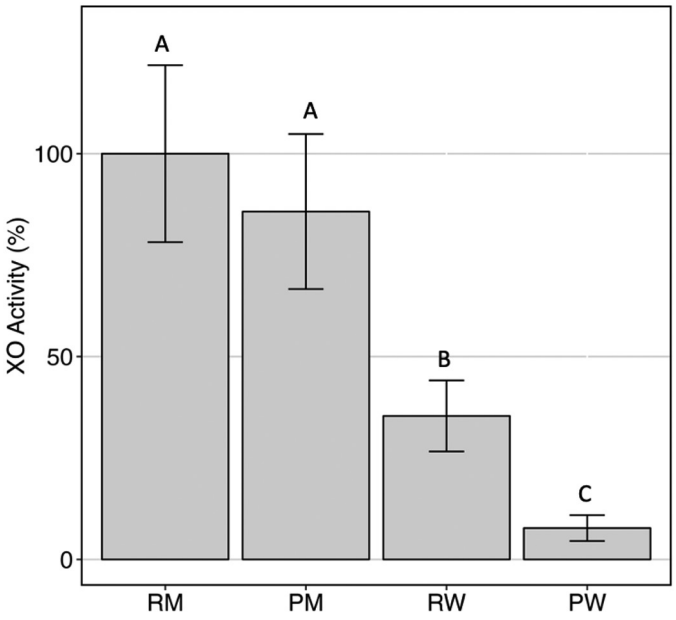

Figure 5. Percent retention (%) of xanthine oxidase (XO) activity for raw milk (RM), pasteurized milk (PM), resulting whey (RW), and pasteurized whey (PW) identified via activity assay. Percent retention has been calculated as the amount of protein activity detected in each sample divided by the amount detected in the control (RM). Error bars represent SD Significantly differing samples have differing uppercase letters (A–C; Tukey's honestly significant difference test, $P < 0.05$).

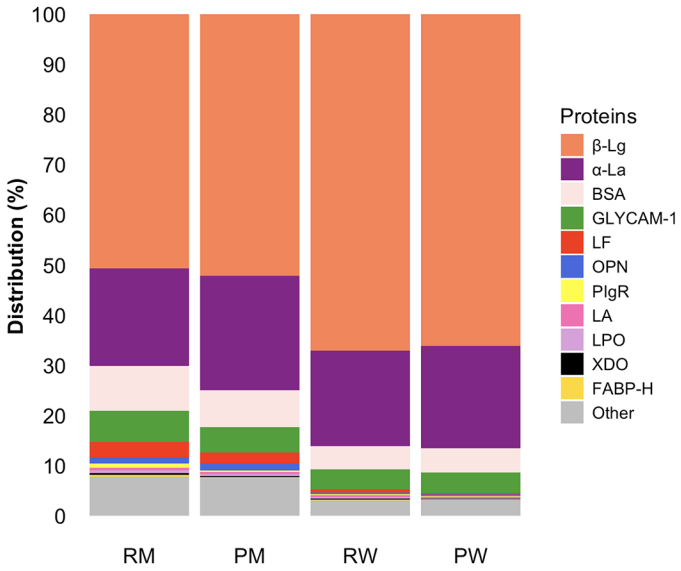

Figure 6. Distribution graph of α-LA, β-LG, BSA, osteopontin (OPN), lactoferrin (LF), lactadherin (LA), fatty acid binding protein-heart (FABP-H), polymeric immunoglobulin receptor (PIgR), xanthine dehydrogenase oxidase (XDO), glycosylation cell adhesion molecule-1 (GLYCAM-1), and other proteins for raw milk (RM), pasteurized milk (PM), resulting whey (RW), and pasteurized whey (PW).

for RW) and another significant decrease from RW to PW whey samples (6%–12% retention for PW; Figure 5). Detection efficiency for XDO/XO ranged from 62% to 107% (Supplemental Table S1).

Xanthine dehydrogenase oxidase/xanthine oxidase is typically found within the MFGM (Ozturk et al., 2019). Therefore, the decrease in activity from PM to RW was consistent with expected results, as fat is removed during the cheesemaking and separation process. Xanthine dehydrogenase oxidase/xanthine oxidase activity in bovine milk has been assessed previously; however, the specific methods used have differed (Sharma et al., 2014; Ozturk et al., 2019; Liu et al., 2020b; Zhang et al., 2021a,b). Our results are partially consistent with those of Zhang et al. (2021a,b), Liu et al. (2020a,b), and Sharma et al. (2014), who observed a significant decrease in XDO/XO activity after heat treatment. However, the decrease from RM to PM in our results was not significant, which aligns with the findings of Ozturk et al. (2019). The decrease in activity from RW to PW suggests the second HTST treatment on the incoming whey stream further reduces the activity of this enzyme.

LC-MS/MS

Proteomics have been used previously to characterize the retention of whey proteins before and after pasteurization of skim and whole bovine milk (Zhang et al., 2016; Yang et al., 2018; Liu et al., 2020b; Wei et al., 2022). However, there is limited proteomics data characterizing the retention of whey proteins before and after commercial HTST pasteurization of milk and no data for the pasteurization of whey post-commercial cheesemaking. The procedure we used to isolate soluble proteins (pH adjustment to 4.6 and centrifugation) before LC-MS/MS allows us to define the identified proteins as soluble proteins (Figure 1).

Changes in Protein Profile from RM to PM. The relative distribution of BSA, GLYCAM-1, LF, PIgR, FABP-H, XDO, LPO, XDO/XO, and LA decreased approximately 1.52%, 1.19%, 0.85%, 0.57%, 0.19%, 0.11%, 0.11%, 0.11%, and 0.09%, respectively, from RM to PM. The relative distribution of α-LA, β-LG, and OPN increased approximately 3.33%, 1.51%, and 0.11%, respectively, from RM to PM (Figure 6; Supplemental Table S3).

A total of 19 proteins were completely lost from RM to PM (of 256 proteins detected in RM), including angiotensinogen, carboxypeptidase B2 (EC:3.4.17.20), tripeptidyl peptidase 1 (EC:3.4.14.9), peroxiredoxin-1, and complement factor C4 (Figure 7; Supplemental Table S4, see Notes). This does not align with the findings of D'Amato et al. (2009), who identified α-enolase (EC:4.2.1.11), carboxypeptidase B2 (EC:3.4.17.20), tripeptidyl peptidase (EC:3.4.14.9), UTP-glucose-1-phosphate-uridyllystransferase (EC:2.7.7.9) and chitinase-3-like

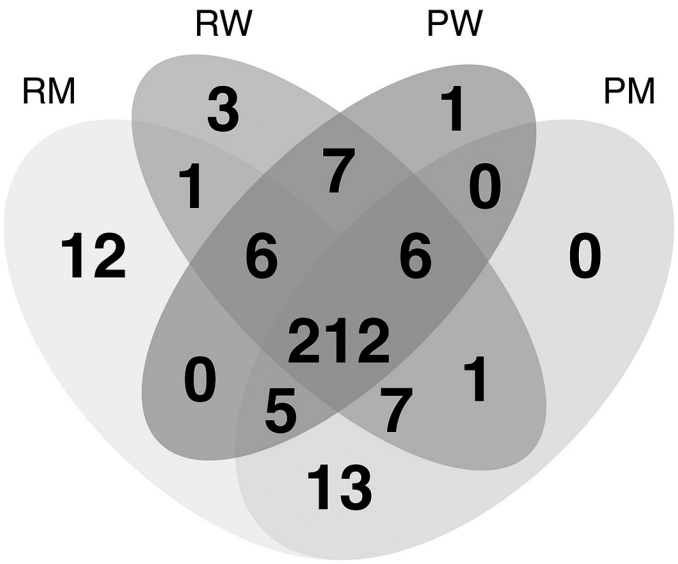

Figure 7. Venn diagram of shared proteins between raw milk (RM), pasteurized milk (PM), resulting whey (RW) and pasteurized whey (PW). Numbers indicate the number of common/shared proteins.

protein in commercially pasteurized whole milk, none of which were identified in our PM samples. However, in their study, they used an enrichment technique to amplify low abundance proteins and dilute major proteins, which may explain the differences in identification (D'Amato et al., 2009).

A total of 43 proteins significantly decreased from RM to PM, including various proteases (e.g., plasminogen and cathepsins B and Z), protease inhibitors (e.g., antithrombin III, α-2-macroglobulin, inter α trypsin inhibitor heavy chain H1 and H4, and factor XIIa inhibitor), immune-related proteins (e.g., haptoglobin; pIgR; complement factors H, C3, C7, C9, and B; Ig like domain containing protein Q1LPG0, Q1MSF6, and Q1LSF02; Ig lambda chain variable region Fragment B9SBR8; and fibrinogen α chain), other enzymes (e.g., LPO, lipoprotein lipase, and thioredoxin), and proteins related to nutrient transport (e.g., BSA, retinol binding protein 4, and FABP-H; Figure 8a; Supplemental Table S5, see Notes). These results align with those of Liu et al. (2020a), who identified (via LC-MS/MS) a significant decrease in an array of proteins (including LPO, haptoglobin, fibrinogen α chain, antithrombin III, and FABP-H) after HTST pasteurization compared with RM. Our results also align with those of Zhang et al. (2021b), who saw a decrease in pIgR, complement factor B, α-2 macroglobulin, haptoglobin, and peptidoglycan recognition protein 1 in their HTST skim milk compared with their RM control.

Lactoferrin numerically decreased from RM to PM by 0.36 log and had a tendency to decrease ($P = 0.054$), but was not significant based on our P-value threshold of 0.05 (Supplemental Table S5). These findings align with the LF ELISA results (Figure 4a), which indicated a decrease after milk pasteurization. Our results for LF partially align with those of Liu et al. (2020a), who saw a significant decrease (via LC-MS/MS) in LF in the serum portion of their HTST-treated milk samples compared with their RM control.

Based on proteomics, some proteins (124) did not significantly decrease from RM to PM, including XDO/XO, β-LG, α-LA, and LA (Supplemental Table S3). The findings for XDO/XO align with the activity assay findings, indicating no change across initial milk pasteurization (Figure 5). Additionally, the findings for β-LG and α-LA align with the SDS-PAGE results, suggesting there was no change in these proteins from RM to PM (Figure 3). These results align with past literature indicating that β-LG and α-LA are thermo-stable at HTST temperatures (Qi et al., 2015; Muuronen et al., 2021; Wazed and Farid, 2022).

Changes in Protein Profile from RW to PW. The relative distribution of β-LG, LF, LA, LPO, XDO/XO, pIgR, and FABP-H decreased approximately 0.95%, 0.51%, 0.17%, 0.16%, 0.11%, 0.06%, and 0.03%, respectively, from RW to PW (Figure 6; Supplemental Table S5). α-Lactalbumin, GLYCAM-1, BSA, and OPN increased 1.36%, 0.25%., 0.19%, and 0.04%, respectively, from PW to RW (Figure 6; Supplemental Table S5).

Twelve proteins were completely lost from RW to PW (of 243 proteins detected in RW), including chymosin, complement factor D, and fibrinogen β-chain (Figure 7; Supplemental Table S4). Beyond this, 17 proteins significantly decreased from RW to PW, including LF, immune-related proteins (e.g., pIgR, complement factor B, and Ig like domain containing protein Q1LPG0), enzymes (e.g., LPO and XDO/XO), nutrient-transporters (e.g., FABP-H, LA, and serotransferrin), antiproteases (e.g., α-2-macroglobulin), and proteases (e.g., prothrombin; Figure 8b; Supplemental Table S6, see Notes). Lactoferrin had the highest log decrease from RW to PW, at 1.38 (Figure 8b; Supplemental Table S6). The proteomics results for LF and XDO/XO align with the decrease we observed via SDS-PAGE (Figure 3), LF ELISA (Figure 4a), and XDO/XO activity assay (Figure 5). We found no previous comparable proteomic-specific studies for sweet whey versus HTST-pasteurized whey.

Changes from PM to RW. The focus of this paper was to examine the effects of pasteurization on milk and whey. However, our data provide insight into changes that resulted from the numerous steps involved in processing PM to RW, including milk preheating, starter culture addition, renneting, addition of calcium chloride, and the partitioning of proteins between the curds and whey (Figure 1; Spalatelu, 2012). Many of these steps

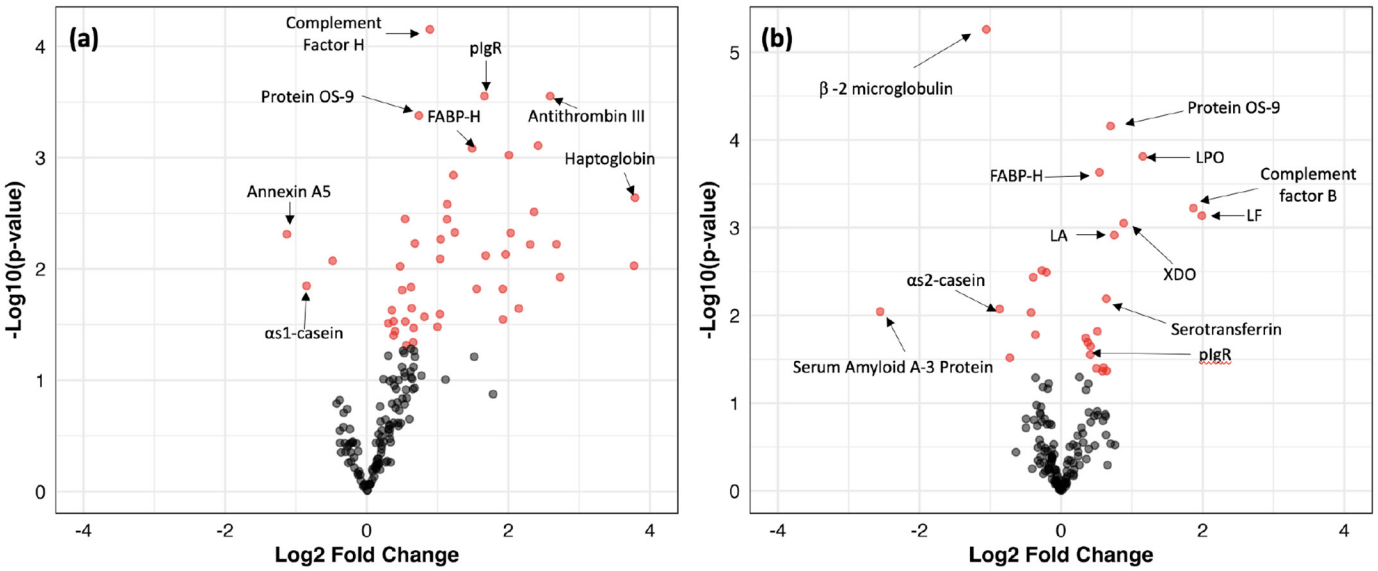

Figure 8. Volcano plots representing the log-fold change in proteins of (a) pasteurized milk (PM) vs. raw milk (RM), and (b) resulting whey (RW) vs. pasteurized whey (PW). Lactoferrin (LF), lactadherin (LA), lactoperoxidase (LPO), fatty acid binding protein-heart (FABP-H), polymeric immunoglobulin receptor (PIgR) and xanthine dehydrogenase oxidase (XDO). Positive values on the x-axis correspond to higher expression of proteins in RM and RW, respectively. Red dots represent proteins that have a log2-fold change that is significantly different ($P < 0.05$), whereas gray and black dots represent proteins that are not significantly different.

can affect protein composition. For example, a decrease in pH due to fermentation can destabilize proteins. Rennet and bacterial proteases can also cause protein degradation. Future studies are necessary to isolate the effects of these factors on whey proteins.

During this multistep process, 19 proteins were completely lost from PM to RW, including procathepsin L, parathyroid hormone-related protein, and histatherin (Figure 7; Supplemental Table S4). Additionally, 24 proteins were significantly reduced from PM to RW, including LF, OPN, various Ig fragments and cathepsin B (Supplemental Table S7, see Notes). The reduction in LF identified via proteomics aligns with the observed decrease in LF from PM to RW identified via ELISA. We could not identify any previous studies that investigated the effect on the proteome of transforming milk into whey and thus could not compare our results to others.

Proteins That Increased in Abundance Across Pasteurization Steps

Three proteins significantly increased from RM to PM: annexin A5, α_{s1}-CN, and CD81 antigen were 0.78, 0.59, and 0.33 log higher in PM than RM, respectively (Figure 8a; Supplemental Table S5). Nine proteins significantly increased from RW to PW. In particular, α_{s1}-CN, α_{s2}-CN, zinc-α-2-glycoprotein, serum amyloid A-3, and β-2 microglobulin were 0.60, 0.25, 0.29, 1.78, and 0.73 log higher in PW than RW, respectively (Figure 8b; Supplemental Table S6).

It is possible that the increase of abundance values from RW to PW for these minor proteins is due to the decrease in abundance of major thermolabile proteins (e.g., LF, LPO, and XDO/XO). This decrease could have led to an increase in ionization efficiency and detection (Page et al., 2007; Liu et al., 2020b; Wei et al., 2022). This theory is evidenced by the higher heat stability of many of these proteins. For example, Tacoma et al. (2017) observed that the abundance of zinc-α-2-glycoprotein had increased in bovine colostrum after heat treatment (60°C for 60 min) and attributed this to the protein's heat stability. Zhang et al. (2021c) observed an increase of β-2 microglobulin in their UHT treated milk (135°C for 15 s) compared with their HTST-pasteurized milk (85°C for 15 s). Additionally, Liu et al. (2020b) observed that β-2 microglobulin was more abundant in the serum fraction of their HTST-treated milk samples than RM samples.

Although caseins are mostly removed during cheesemaking and whey protein isolation, some intact casein and casein fragments remain in the whey (Wei et al., 2022). The observed increase in α_{s1}-CN from RM to PM and increase in α_{s1}- and α_{s2}-CN from RW to PW represent an increase in detection of tryptic peptides from intact proteins, not smaller fragments. We employed ethanol precipitation to isolate intact proteins from small peptides before trypsin digestion to focus on the survival of intact proteins across the pasteurization steps. The observed increase in these caseins across heat treatments likely represents decreased interference from other proteins that were lost in pasteurization. Liu et al. (2020b) also

observed an increase in abundance of casein in the serum fraction of their HTST-treated milk samples relative to their RM control and posited that the increase could be due to a decrease in other serum proteins and an increase in heat-stable caseins.

Future proteomics work could apply depletion strategies for abundant proteins (β-LG, α-LA, BSA) to better compare the abundance of low abundant whey proteins before and after heat treatment (D'Amato et al., 2009; Fonslow et al., 2011; Altomare et al., 2016).

CONCLUSIONS

This study showed that commercial-scale HTST pasteurization of milk and whey induces whey protein denaturation and, therefore, loss of thermolabile intact whey proteins. The loss of these whey proteins was observed both after HTST pasteurization of RM (before cheesemake) and after HTST pasteurization of the RW (before concentration and evaporation to powder). A strength of this study is that it examined samples from commercial-scale processes. The impact of HTST processing may be mitigated using alternative processing methods (e.g., high pressure processing, UV C irradiation, and microfiltration) on RM or whey streams, with the aim to create a higher value product. Additionally, dairy producers can fractionate select bioactive proteins (LF, IgA, IgM, XDO/XO, and LPO) upstream of cheese-make to better preserve their bioactivity for use in high value products.

NOTES

This research was funded by BUILD Dairy (Logan, UT) and Hilmar Cheese Company (Hilmar, CA). We thank Hilmar Cheese Company for providing samples for the study and the Mass Spectrometry Center at Oregon State University (Corvallis, OR) for providing the instrumentation we used (supported by the National Institute of Health grant #1S10OD020111-01). Supplemental material for this article is available at https://figshare.com/projects/HTST_PASTEURIZATION_EFFECTS_ON_MILK_AND_WHEY/220342. No human or animal subjects were used, so this analysis did not require approval by an Institutional Animal Care and Use Committee or Institutional Review Board. The authors have not stated any conflicts of interest.

Nonstandard abbreviations used: ACN = acetonitrile; ANS = anilinonaphthalene-1-sulfonic acid; BCA = bicinchoninic acid; CCP = critical control point; DTT = dithiothreitol; FA = formic acid; FABP-H = fatty acid binding protein-heart; GLYCAM-1: glycosylation-dependent cell adhesion molecule-1; LA = lactadherin; LC-MS/MS = liquid chromatography tandem MS; LF = lactoferrin; MFGM = milk fat globular membrane; NR = nonreducing; OPN = osteopontin; pIgR = polymeric immunoglobulin receptor; PM = pasteurized milk; PMO = Pasteurized Milk Ordinance; PW = pasteurized whey; R = reducing; RFI = relative fluorescent intensity; RM = raw milk; RW = resulting whey; S_0 = hydrophobicity index; SFS = soluble fraction sample; WPC = whey protein concentrate; WS = whole sample; XDO/XO = xanthine dehydrogenase oxidase and xanthine oxidase; λ em = emission wavelength; λ ex = excitation wavelength.

REFERENCES

Alizadeh-Pasdar, N., and E. C. Li-Chan. 2000. Comparison of protein surface hydrophobicity measured at various pH values using three different fluorescent probes. J. Agric. Food Chem. 48:328–334. https://doi.org/10.1021/jf990393p.

Allen, M. D. 2010. A comparison of analytical methods for quantifying denatured whey proteins and their correlation to solubility. MS thesis. Dairy Science Department, California Polytechnic State University.

Altomare, A., E. Fasoli, M. Colzani, X. M. Paredes Parra, M. Ferrari, F. Cilurzo, C. Rumio, L. Cannizzaro, M. Carini, and P. G. Righetti. 2016. An in depth proteomic analysis based on ProteoMiner, affinity chromatography and nano-HPLC–MS/MS to explain the potential health benefits of bovine colostrum. J. Pharm. Biomed. Anal. 121:297–306. https://doi.org/10.1016/j.jpba.2016.01.013.

Anandharamakrishnan, C., C. Rielly, and A. Stapley. 2007. Effects of process variables on the denaturation of whey proteins during spray drying. Dry. Technol. 25:799–807. https://doi.org/10.1080/07373930701370175.

Andoyo, R., V. Dianti Lestari, E. Mardawati, and B. Nurhadi. 2018. Fractal dimension analysis of texture formation of whey protein-based foods. Int. J. Food Sci. 2018:7673259. https://doi.org/10.1155/2018/7673259.

Atamer, Z., M. Samtlebe, H. J. Neve, K. Heller, and J. Hinrichs. 2013. Elimination of bacteriophages in whey and whey products. Front. Microbiol. 4:191. https://doi.org/10.3389/fmicb.2013.00191.

Bernal, V., and P. Jelen. 1985. Thermal stability of whey proteins—A calorimetric study. J. Dairy Sci. 68:2847–2852. https://doi.org/10.3168/jds.S0022-0302(85)81177-2.

Beyaztaş, S., and O. Arslan. 2015. Purification of xanthine oxidase from bovine milk by affinity chromatography with a novel gel. J. Enzyme Inhib. Med. Chem. 30:442–447. https://doi.org/10.3109/14756366.2014.943204.

Bogahawaththa, D., R. Buckow, J. Chandrapala, and T. Vasiljevic. 2018. Comparison between thermal pasteurization and high pressure processing of bovine skim milk in relation to denaturation and immunogenicity of native milk proteins. Innov. Food Sci. Emerg. Technol. 47:301–308. https://doi.org/10.1016/j.ifset.2018.03.016.

Bogahawaththa, D., J. Chandrapala, and T. Vasiljevic. 2017. Thermal denaturation of bovine immunoglobulin G and its association with other whey proteins. Food Hydrocoll. 72:350–357. https://doi.org/10.1016/j.foodhyd.2017.06.017.

Bogahawaththa, D., and T. Vasiljevic. 2020. Denaturation of selected bioactive whey proteins during pasteurization and their ability to modulate milk immunogenicity. J. Dairy Res. 87:484–487. https://doi.org/10.1017/S0022029920000989.

Briggiler Marcó, M. B., and D. J. Mercanti. 2021. Bacteriophages in dairy plants. Adv. Food Nutr. Res. 97:1–54. https://doi.org/10.1016/bs.afnr.2021.02.015.

Burrington, K., and S. Agrawal. 2012. Technical report: Whey protein heat stability. US Dairy Export Council, Arlington, VA.

Chandrapala, J., M. C. Duke, S. R. Gray, B. Zisu, M. Weeks, M. Palmer, and T. Vasiljevic. 2015. Properties of acid whey as a function of pH and temperature. J. Dairy Sci. 98:4352–4363. https://doi.org/10.3168/jds.2015-9435.

D'Amato, A., A. Bachi, E. Fasoli, E. Boschetti, G. Peltre, H. Senechal, and P. G. Righetti. 2009. In-depth exploration of cow's whey proteome via combinatorial peptide ligand libraries. J. Proteome Res. 8:3925–3936. https://doi.org/10.1021/pr900221x.

Davoodi, S. H., R. Shahbazi, S. Esmaeili, S. Sohrabvandi, A. Mortazavian, S. Jazayeri, and A. Taslimi. 2016. Health-related aspects of milk proteins. Iran J. Pharm. Res. 15:573–591.

De Wit, J., and T. Van Kessel. 1996. Effects of ionic strength on the solubility of whey protein products. A colloid chemical approach. Food Hydrocoll. 10:143–149. https://doi.org/10.1016/S0268-005X(96)80028-2.

Deeth, H. C. 2021. Heat-induced inactivation of enzymes in milk and dairy products. A review. Int. Dairy J. 121:105104. https://doi.org/10.1016/j.idairyj.2021.105104.

Dissanayake, M., and T. Vasiljevic. 2009. Functional properties of whey proteins affected by heat treatment and hydrodynamic high-pressure shearing. J. Dairy Sci. 92:1387–1397. https://doi.org/10.3168/jds.2008-1791.

Early, R. 2012. Dairy products and milk-based food ingredients. Pages 417–445 in Natural Food Additives, Ingredients and Flavourings. D. Baines and R. Seal, ed. Elsevier.

Edwards, P. J., and G. B. Jameson. 2014. Structure and stability of whey proteins. Pages 201–242 in Milk Proteins. 2nd ed. H. Singh, M. Boland, and A. Thompson, ed. Academic Press, San Diego, CA.

Farkye, N. 2002. Enzymes indigenous to milk | Xanthine Oxidase.

FDA (Food and Drug Administration). 2019. Grade "A" Pasteurized Milk Ordinance. Accessed Jun. 1, 2024. https://www.fda.gov/media/140394/download.

FDA (Food and Drug Administration). 2024. 21 CFR 184.1979c Whey Protein Concentrate. § 184.1979 c(b)(3). https://www.ecfr.gov/current/title-21/chapter-I/subchapter-B/part-184/subpart-B/section-184.1979c.

Fonslow, B. R., P. C. Carvalho, K. Academia, S. Freeby, T. Xu, A. Nakorchevsky, A. Paulus, and J. R. Yates III.. 2011. Improvements in proteomic metrics of low abundance proteins through proteome equalization using ProteoMiner prior to MudPIT. J. Proteome Res. 10:3690–3700. https://doi.org/10.1021/pr200304u.

Freire, P., A. Zambrano, A. Zamora, and M. Castillo. 2022. Thermal denaturation of milk whey proteins: A comprehensive review on rapid quantification methods being studied, developed and implemented. Dairy 3:500–512. https://doi.org/10.3390/dairy3030036.

Gorevic, P. D., F. C. Prelli, and B. Frangione. 1985. [1] Immunoglobulin G (IgG). Methods Enzymol. 116:3–25. https://doi.org/10.1016/S0076-6879(85)16003-9.

Grácia-Juliá, A., M. René, M. Cortés-Muñoz, L. Picart, T. López-Pedemonte, D. Chevalier, and E. Dumay. 2008. Effect of dynamic high pressure on whey protein aggregation: A comparison with the effect of continuous short-time thermal treatments. Food Hydrocoll. 22:1014–1032. https://doi.org/10.1016/j.foodhyd.2007.05.017.

Hurley, W. L., and P. K. Theil. 2011. Perspectives on immunoglobulins in colostrum and milk. Nutrients 3:442–474. https://doi.org/10.3390/nu3040442.

IMNRC (Institute of Medicine National Research Council). 2003. Scientific Criteria to Ensure Safe Food. National Academies Press, Washington, DC.

Johansen, F. E., R. Braathen, and P. Brandtzaeg. 2000. Role of J chain in secretory immunoglobulin formation. Scand. J. Immunol. 52:240–248. https://doi.org/10.1046/j.1365-3083.2000.00790.x.

Joyce, A. M., A. L. Kelly, and J. A. O'Mahony. 2018. Controlling denaturation and aggregation of whey proteins during thermal processing by modifying temperature and calcium concentration. Int. J. Dairy Technol. 71:446–453. https://doi.org/10.1111/1471-0307.12507.

Kelly, A. L., T. Huppertz, and J. J. Sheehan. 2008. Pre-treatment of cheese milk: principles and developments. Dairy Sci. Technol. 88:549–572. https://doi.org/10.1051/dst:2008017.

Kilara, A. 2015. Whey and whey products. Pages 349–366 in Dairy Processing and Quality Assurance. R. C. Chandan, A. Kilara, and N. P. Shah, ed. Wiley Blackwell.

Kim, B. J., J. Koh, N. Liang, J. Yang, G. Ozturk, D. Barile, and D. C. Dallas. 2023. Effect of vat pasteurization, ultra-high temperature sterilization, retort sterilization and homogenization on soluble proteins in donor human milk detected via proteomics. Lebensm. Wiss. Technol. 182:114842. https://doi.org/10.1016/j.lwt.2023.114842.

Kummer, A., D. Kitts, E. Li-Chan, J. Losso, B. Skura, and S. Nakai. 1992. Quantification of bovine IgG in milk using enzyme-linked immunosorbent assay. Food Agric. Immunol. 4:93–102. https://doi.org/10.1080/09540109209354757.

Latypov, R. F., D. Liu, K. Gunasekaran, T. S. Harvey, V. I. Razinkov, and A. A. Raibekas. 2008. Structural and thermodynamic effects of ANS binding to human interleukin-1 receptor antagonist. Protein Sci. 17:652–663. https://doi.org/10.1110/ps.073332408.

Li, H., T. Zhao, H. Li, and J. Yu. 2021. Effect of heat treatment on the property, structure, and aggregation of skim milk proteins. Front. Nutr. 8:714869. https://doi.org/10.3389/fnut.2021.714869.

Liu, Y., L. Xiong, E. Kontopodi, S. Boeren, L. Zhang, P. Zhou, and K. Hettinga. 2020a. Changes in the milk serum proteome after thermal and non-thermal treatment. Innov. Food Sci. Emerg. Technol. 66:102544. https://doi.org/10.1016/j.ifset.2020.102544.

Liu, Y., W. Zhang, L. Zhang, K. Hettinga, and P. Zhou. 2020b. Characterizing the changes of bovine milk serum proteins after simulated industrial processing. Lebensm. Wiss. Technol. 133:110101. https://doi.org/10.1016/j.lwt.2020.110101.

Mainer, G., L. Sanchez, J. Ena, and M. Calvo. 1997. Kinetic and thermodynamic parameters for heat denaturation of bovine milk IgG, IgA and IgM. J. Food Sci. 62:1034–1038. https://doi.org/10.1111/j.1365-2621.1997.tb15032.x.

Masterson, H. K., T. F. O'Callaghan, M. O'Donovan, J. P. Murphy, K. Sugrue, R. A. Owens, and R. M. Hickey. 2024. Relative quantitative proteomic profiling of bovine colostrum and transition milk at onset of lactation. Int. Dairy J. 148:105804. https://doi.org/10.1016/j.idairyj.2023.105804.

Meunier-Goddik, L., and S. Sandra. 2011. LIQUID MILK PRODUCTS | Liquid Milk Products: Pasteurized Milk. https://doi.org/10.1016/b978-0-12-374407-4.00280-6.

Morr, C. 1987. Effect of HTST pasteurization of milk, cheese whey and cheese whey UF retentate upon the composition, physicochemical and functional properties of whey protein concentrates. J. Food Sci. 52:312–317. https://doi.org/10.1111/j.1365-2621.1987.tb06601.x.

Mullan, M. 2015. HTST pasteurization. Is it time to raise statutory time/temperature conditions to destroy *Mycobacterium avium* subsp. *paratuberculosis* (MAP)?

Muuronen, K., R. Partanen, H.-J. Heidebrecht, and U. Kulozik. 2021. Effects of conventional processing methods on whey proteins in production of native whey powder. Int. Dairy J. 116:104959. https://doi.org/10.1016/j.idairyj.2020.104959.

Nezlin, R. 2019. Dynamic aspects of the immunoglobulin structure. Immunol. Invest. 48:771–780. https://doi.org/10.1080/08820139.2019.1597110.

Ng, W. C., V. Wong, B. Muller, G. Rawlin, and L. E. Brown. 2010. Prevention and treatment of influenza with hyperimmune bovine colostrum antibody. PLoS One 5:e13622. https://doi.org/10.1371/journal.pone.0013622.

O'Regan, J., M. Ennis, and D. Mulvihill. 2009. Milk proteins. Pages 298–358 in Handbook of Hydrocolloids. 2nd ed. G. O. Phillips and P. A. Williams, ed. Elsevier.

Olson, B. J. 2016. Assays for determination of protein concentration. Curr. Protoc. Pharmacol. 73:A.3A.1–A.3A.32. https://doi.org/10.1002/cpph.3.

Özer, B. 2014. Natural Anti-Microbial Systems | Lactoperoxidase and Lactoferrin.

Ozturk, G., J. B. German, and J. M. de Moura Bell. 2019. Effects of industrial heat treatments on the kinetics of inactivation of antimicrobial bovine milk xanthine oxidase. NPJ Sci. Food 3:13. https://doi.org/10.1038/s41538-019-0046-8.

Page, J. S., R. T. Kelly, K. Tang, and R. D. Smith. 2007. Ionization and transmission efficiency in an electrospray ionization—mass spectrometry interface. J. Am. Soc. Mass Spectrom. 18:1582–1590. https://doi.org/10.1016/j.jasms.2007.05.018.

Panthi, R. R., K. N. Jordan, A. L. Kelly, and J. D. Sheehan. 2017. Selection and treatment of milk for cheesemaking. Pages 23–50 in Cheese: Chemistry, Physics, and Microbiology. 4th ed. P. L. H. McSweeney, P. F. Fox, P. D. Cotter, and D. W. Everett, ed. Elsevier.

Patel, A. S., C. Yeung, C. Brennan, and H. Zheng. 2022. Ingredients and Formulation.
Pearce, R. J. 1992. Whey processing. Pages 73–89 in Whey and Lactose Processing. J. G. Zadow, ed. Springer Dordrecht.
Pelegrine, D., and C. Gasparetto. 2005. Whey proteins solubility as function of temperature and pH. Lebensm. Wiss. Technol. 38:77–80. https://doi.org/10.1016/j.lwt.2004.03.013.
Pires, A. F., N. G. Marnotes, O. D. Rubio, A. C. Garcia, and C. D. Pereira. 2021. Dairy by-products: A review on the valorization of whey and second cheese whey. Foods 10:1067. https://doi.org/10.3390/foods10051067.
Qi, P. X., D. Ren, Y. Xiao, and P. M. Tomasula. 2015. Effect of homogenization and pasteurization on the structure and stability of whey protein in milk. J. Dairy Sci. 98:2884–2897. https://doi.org/10.3168/jds.2014-8920.
Qian, F., J. Sun, D. Cao, Y. Tuo, S. Jiang, and G. Mu. 2017. Experimental and modelling study of the denaturation of milk protein by heat treatment. Korean J. Food Sci. Anim. Resour. 37:44–51. https://doi.org/10.5851/kosfa.2017.37.1.44.
Ryan, K. N., Q. Zhong, and E. A. Foegeding. 2013. Use of whey protein soluble aggregates for thermal stability—A hypothesis paper. J. Food Sci. 78:R1105–R1115. https://doi.org/10.1111/1750-3841.12207.
Rynne, N. M., T. P. Beresford, A. L. Kelly, and T. P. Guinee. 2004. Effect of milk pasteurization temperature and in situ whey protein denaturation on the composition, texture and heat-induced functionality of half-fat Cheddar cheese. Int. Dairy J. 14:989–1001. https://doi.org/10.1016/j.idairyj.2004.03.010.
Schuck, P., R. Jeantet, B. Bhandari, X. D. Chen, Í. T. Perrone, A. F. de Carvalho, M. Fenelon, and P. Kelly. 2016. Recent advances in spray drying relevant to the dairy industry: A comprehensive critical review. Dry. Technol. 34:1773–1790. https://doi.org/10.1080/07373937.2016.1233114.
Sharma, P., I. Oey, P. Bremer, and D. W. Everett. 2014. Reduction of bacterial counts and inactivation of enzymes in bovine whole milk using pulsed electric fields. Int. Dairy J. 39:146–156. https://doi.org/10.1016/j.idairyj.2014.06.003.
Sharma, P., I. Oey, and D. W. Everett. 2016. Thermal properties of milk fat, xanthine oxidase, caseins and whey proteins in pulsed electric field-treated bovine whole milk. Food Chem. 207:34–42. https://doi.org/10.1016/j.foodchem.2016.03.076.
Spalatelu, C. 2012. Biotechnological valorisation of whey. Innov. Rom. Food Biotechnol. 10:1.
Tacoma, R., S. Gelsinger, Y. Lam, R. Scuderi, D. Ebenstein, A. Heinrichs, and S. Greenwood. 2017. Exploration of the bovine colostrum proteome and effects of heat treatment time on colostrum protein profile. J. Dairy Sci. 100:9392–9401. https://doi.org/10.3168/jds.2017-13211.
USDA. 2012. General Specifications for Dairy Plants Approved for USDA Inspection and Grading Service. § 7 CFR §58.809. Accessed Jun. 1, 2024. https://www.ams.usda.gov/sites/default/files/media/General%20Specifications%20for%20Dairy%20Plants%20Approved%20for%20USDA%20Inspection%20and%20Grading%20Service.pdf.
USDEC (US Dairy Export Council). 2004. Reference manual for US whey and lactose products. Accessed Jun. 15, 2024. https://usdec.files.cms-plus.com/PDFs/2008ReferenceManuals/Whey_Lactose_Reference_Manual_Complete2_Optimized.pdf.
Wazed, M. A., and M. Farid. 2022. Denaturation kinetics and storage stability of Osteopontin in reconstituted infant milk formula. Food Chem. 379:132138. https://doi.org/10.1016/j.foodchem.2022.132138.
Wazed, M. A., M. Ismail, and M. Farid. 2020. Pasteurized ready-to-feed (RTF) infant formula fortified with lactoferrin: A potential niche product. J. Food Eng. 273:109810. https://doi.org/10.1016/j.jfoodeng.2019.109810.
Webb, B. H., and E. O. Whittier. 1948. The utilization of whey: A review. J. Dairy Sci. 31:139–164. https://doi.org/10.3168/jds.S0022-0302(48)92188-2.
Wei, Z., J. Kang, M. Liao, H. Ju, R. Fan, J. Shang, X. Ning, and M. Li. 2022. Investigating changes of proteome in the bovine milk serum after retort processing using proteomics techniques. Food Sci. Nutr. 10:307–316. https://doi.org/10.1002/fsn3.2300.
Wittwer, M., P. Hammer, M. Runge, P. Valentin-Weigand, H. Neubauer, K. Henning, and K. Mertens-Scholz. 2022. Inactivation kinetics of *Coxiella burnetii* during high-temperature short-time pasteurization of milk. Front. Microbiol. 12:753871. https://doi.org/10.3389/fmicb.2021.753871.
Yang, Y., N. Zheng, X. Zhao, J. Yang, Y. Zhang, R. Han, Y. Qi, S. Zhao, S. Li, F. Wen, T. Guo, C. Zang, and J. Wang. 2018. Changes in bovine milk fat globule membrane proteins caused by heat procedures using a label-free proteomic approach. Food Res. Int. 113:1–8. https://doi.org/10.1016/j.foodres.2018.06.046.
Zhang, L., S. Boeren, M. Smits, T. van Hooijdonk, J. Vervoort, and K. Hettinga. 2016. Proteomic study on the stability of proteins in bovine, camel, and caprine milk sera after processing. Food Res. Int. 82:104–111. https://doi.org/10.1016/j.foodres.2016.01.023.
Zhang, W., Y. Liu, Z. Li, S. Xu, K. Hettinga, and P. Zhou. 2021a. Retaining bioactive proteins and extending shelf life of skim milk by microfiltration combined with Ultraviolet-C treatment. Lebensm. Wiss. Technol. 141:110945. https://doi.org/10.1016/j.lwt.2021.110945.
Zhang, W., Y. Liu, Z. Li, S. Xu, J. Zhang, K. Hettinga, and P. Zhou. 2021b. Effects of microfiltration combined with ultrasonication on shelf life and bioactive protein of skim milk. Ultrason. Sonochem. 77:105668. https://doi.org/10.1016/j.ultsonch.2021.105668.
Zhang, Y., L. Min, S. Zhang, N. Zheng, D. Li, Z. Sun, and J. Wang. 2021c. Proteomics analysis reveals altered nutrients in the whey proteins of dairy cow milk with different thermal treatments. Molecules 26:4628. https://doi.org/10.3390/molecules26154628.

ORCIDS

Joanna Haas, https://orcid.org/0009-0002-0425-4852
David C. Dallas https://orcid.org/0000-0002-9696-0967